Published in final edited form as:
Cardiovasc Pathol. 2013 January ; 22(1): 91–95. doi:10.1016/j.carpath.2012.03.005.

Lack of Thrombospondin-2 Reduces Fibrosis and Increases Vascularity Around Cardiac Cell Grafts

Hans Reinecke[1], **Thomas E. Robey**[2], **John Mignone**[3], **Veronica Muskheli**[1], **Paul Bornstein**[4], and **Charles E. Murry**[1,2,3]

[1]Department of Pathology, Center for Cardiovascular Biology and Institute for Stem Cell and Regenerative Medicine, University of Washington, Seattle, WA 98109.

[2]Department of Bioengineering, University of Washington, Seattle, WA 98195.

[3]Department of Medicine/Cardiology, University of Washington, Seattle, WA 98195.

[4]Department of Biochemistry, University of Washington, Seattle, WA 98195.

Abstract

Background—Fibrosis around cardiac cell injections represents an obstacle to graft integration in cell-based cardiac repair. Thrombospondin-2 (TSP-2) is a pro-fibrotic, anti-angiogenic matricellular protein and an attractive target for therapeutic knockdown to improve cardiac graft integration and survival.

Methods—We used a TSP-2 knockout (KO) mouse in conjunction with a fetal murine cardiomyocyte grafting model to evaluate the effects of a lack of TSP-2 on fibrosis, vascular density and graft size in the heart.

Results—Two weeks after grafting in the uninjured heart, fibrosis area was reduced 4.5-fold in TSP-2 KO mice and the thickness of the peri-graft scar capsule was reduced 7-fold compared to wild-type (WT). Endothelial cell density in the peri-graft region increased 2.5-fold in the absence of TSP-2, and cardiomyocyte graft size increased by 46% in TSP-2 KO hearts.

Conclusions—TSP-2 is a key regulator of fibrosis and angiogenesis following cell grafting in the heart, and its absence promotes better graft integration, vascularization and survival.

Introduction

Several cell types form grafts in the heart, some of which have been shown to improve contractile function of the infarcted heart (1-3). Fibrosis is a problem for cell-based cardiac repair; scar that rapidly isolates grafted cells from host myocardium remains a major barrier to graft integration (4, 5). The scarring response to injury in the heart is regulated by matricellular proteins poised to respond to stress (6). One such protein, TSP-2, has been

Address for Correspondence: Charles E. Murry, MD, PhD Center for Cardiovascular Biology and Institute for Stem Cell and Regenerative Medicine University of Washington 815 Mercer Street Seattle, WA 98109 Phone: 206-616-8685 Fax: 206-897-1540 murry@uw.edu.

Disclosures
None

implicated as a controller of scar formation and blood vessel growth, both in response to skin wounding and to the implantation of subcutaneous biomaterials (7-10).

The TSP-2 KO mouse has disorganized collagen fibrils (11), altered collagen fiber packing (12) in uninjured tissues, increased angiogenesis (7), and disordered collagen in wounds (13). Known phenotypes for TSP-2 KO mice in the heart include a defect in cardiac tensile strength, leading to cardiac rupture following angiotensin II stress (14) or infarction (15). TSP-2 expression increases in the fibrosis-prone hypertensive heart (16), and thrombospondin homologues have been implicated in cardiac repair (17). We hypothesized that TSP-2 promotes fibrosis and inhibits angiogenesis following cell transplantation in the heart and tested this hypothesis in TSP-2 KO mice.

Materials and Methods

Animals

TSP-2 KO mice were generated by Kyriakides et al. (11) (available from Jackson Laboratories; Bar Harbor, ME). The procedure replaced exons 2 (including the translation start site) and 3 with PGK-Neo and PGK-TK cassettes. The resulting male chimeras were mated with C57BL/6 females, and heterozygotes were then serially bred with 129SvJ mice to produce homozygous TSP-2-null mice on a homogeneous 129 background (11). Both wild type and homozygous knockout mice are fertile. Each breeder animal was genotyped to verify experimental grouping. Animals were housed under specific pathogen-free conditions and used in accordance with NIH guidelines. The Institutional Animal Care and Use Committee at the University of Washington approved this study according to UW IACUC protocol #2225-04.

Surgery

Our surgical procedure involved grafting fetal mouse cardiomyocytes into syngeneic hosts. To distinguish grafted from host cells, cells were labeled with bromodeoxyuridine (BrdU), a thymidine analog that is incorporated into DNA during DNA synthesis. After verifying pregnancy by ultrasound, we labeled embryonic heart cells *in utero* by injecting 2 mg (0.2 ml of 10 mg/ml stock solution) of BrdU into timed pregnant females at embryonic day (E) 13, E13.5, E14, and E14.5, with the last injection 1 hour before harvest. Midline intraperitoneal injections were administered after palpating the bicornuate uterus. E14.5 pregnant females were anesthetized with an intraperitoneal injection of 20 μl/g body weight Avertin (20 mg/ml). After embryo collection, the females were euthanized using sodium pentabarbitol. Fetal hearts were excised under a dissecting microscope and washed in ice-cold ADS buffer(120 mMNaCl, 20 mM HEPES, 8 mM NaH_2PO_4, 6 mM glucose, 5 mM KCl, 0.8 mM $MgSO_4$, pH 7.4).

Hearts were minced into ~1 mm^2 pieces and subjected to 2-3 serial 30 min trypsin incubations at 37°C in a shaking waterbath. The trypsin digest solution consisted of 0.1% trypsin (Invitrogen; Carlsbad, CA), 10 mM HEPES (Invitrogen), 100 μg/ml penicillin/ streptomycin (Invitrogen) and 200 U/ml DNAse (Invitrogen) in ADS buffer. Isolated cells were washed, counted, assessed for viability (cells from each phenotype were about 90% viable by trypan blue exclusion), and concentrated for injection. Each E14.5 heart yielded about 200,000 cells. Some cells were plated on gelatin-coated chamber slides at 100,000 cells per well for assessment of BrdU labeling and myocyte purity. These cells were permitted to attach in DMEM with 20% FBS overnight and allowed to grow for an additional day before being washed in PBS and fixed in ice-cold methanol. After plating cells in chamber slides, some non-viable floating cells were observed, but a large number of the plated cells attached and spread into the characteristic morphology of primary

cardiomyocytes. 1×10^5 cardiomyocytes were suspended in a volume of 5 μl of serum- and antibiotics-free DMEM (Invitrogen) and maintained on ice until injection.

Mice were prepared for cardiac cell injection after left-sided thoracotomy, as previously described (18, 19). Mice were anesthetized with an intraperitoneal injection of 20 μl/g body weight Avertin (20 mg/ml), kept warm on a water recirculating heating pad and orotracheally intubated for ventilation with 100% oxygen at 13-16 cm H_2O with 3 cm H_2O of PEEP and a rate of 165 breaths per min. The chest was opened, proper lung inflation assessed and the pericardial membrane was reflected from the surface of the heart. One 5 μl injection from a 30 gauge needle, using a 10 μl Hamilton syringe (Hamilton Corp.; Reno, NV), was delivered 1 mm medial to the left anterior descending coronary artery (LAD). TSP-2 KO cells were grafted into TSP-2 KO mice and wild-type (WT) cells into WT recipients. The chest wall was then closed with mattress sutures using 6-0 polypropylene sutures. Muscle fascia and skin wounds were restored in the same manner and the mouse was hydrated with 0.5 ml subcutaneously delivered isotonic saline. A sub-population of prepared cells was cultured to identify cardiomyocyte purity and BrdU labeling efficiency.

Table 1 summarizes the study groups. In total, 115 recipient mice and 21 pregnant females were used in this study. Overall, post-surgical mortality was similar between WT and TSP-KO mice 82% vs. 78%, respectively). The 10 sham group mice (5 per genotype) that were subjected to an open thoracotomy without injection were used for baseline collagen and blood vessel measurements. Hearts were removed from sodium pentabarbitol-overdosed (200 mg/kg) mice 2 weeks after grafting and fixed in Methyl Carnoy's (MC) fixative or prepared for frozen sections after dehydrating the tissue through sucrose gradient. MC-fixed hearts were cut into 2-mm thick sections and processed progressively through sequential xylene dehydration and embedded in paraffin for later sectioning into 5-μm paraffin sections. 7-μm frozen sections were taken from OCT-embedded 2 mm thick heart slices.

Histology

Tissue morphology and extent of fibrosis were determined from hematoxylin and eosin and Picrosirius red-stained sections. Immunostaining of MC-fixed, paraffin-embedded hearts used commercially available antibodies, except for the anti-TSP-2 IgG. This rabbit polyclonal antibody was affinity-purified by incubation of the antibody preparations with TSP-2 immobilized on nitrocellulose and eluted with 0.1 M glycine-HCl, pH 2.6. The titers of antibody preparations were determined by Western blot analysis of known amounts of TSP-2 with differing antibody dilutions (11). When used on cardiac sections, the TSP-2 IgG antibody was diluted at 1:1000. Anti-myosin heavy chain diluted 1:100 (clone MF20 Developmental Studies Hybridoma Bank; Iowa City, IA), anti-pan-N-cadherin IgG diluted 1:500 (Sigma; St. Louis, MO), and anti-BrdU-POD diluted 1:40 (Roche; Temecula, CA) were used to identify the character and extent of the grafted cells. Immunostaining with anti-CD31, diluted at 1:500 (BD Pharmingen; San Jose, CA), of frozen sections indicated angiogenic responses to grafted cells. Graft fibrosis was measured from sections first immunostained for BrdU and counterstained with hematoxylin, and then further counterstained for 30 min with Picrosirius red and and Fast green.

The inclusion criteria for countable grafts consisted of several contiguous BrdU positive cells per section. Occasionally, multiple small grafts could be counted per animal. In that case, average values were calculated for each animal, using all of the grafts. This value represented each animal in subsequent calculations. Scar thickness and area were measured from SR-stained sections using Image J (NIH; Bethesda, MD) morphometry software. Vessel density was measured using pixel thresholding in Photoshop (Adobe; San Jose, CA), and a grid-based CD31+ vessel profile count for vascular index. Graft size was quantified by counting the number of BrdU-positive cells per 5-μm section. Total scar fibrosis (including

the needle tract injury) was calculated using pixel thresholding in Photoshop from entire sections of Picrosirius red- and Fast green-counterstained heart sections in the section where grafts were identified. Quantitative data for graft size and scar morphometry were collected from MC-fixed hearts with grafts. The area occupied by CD31 staining was quantified in grafted regions of diaminobenzadine-stained adjacent sections where grafts were observed. All counting and analysis were done by a single observer in a blinded fashion. Statistical significance was determined using a two tailed, unequal variance Student's T-test. All values are presented as mean ± SEM.

Quantitative PCR (qPCR) for mouse collagen type I alpha 1 (Col1a1)

To quantify mouse Col1a1 mRNA after cardiomyocyte transplantation, neonatal mouse cardiomyocytes from WT and TSP-2 KO mice were isolated, preplated to remove contaminating fibroblasts, labeled with Vybrant DiI (Invitrogen) and immediately injected into the uninjured hearts of WT and TSP-2 KO mice, respectively, at 5×10^5 per heart (n=6 per group). Four days after cell transplantation, hearts were harvested and the DiI-positive injection sites visualized with a fluorescence-equipped stereomicroscope (Nikon SMZ). The DiI-positive areas were harvested and snap-frozen. RNA was isolated using the RNeasy fibrous tissue kit (Qiagen). For each sample, 500 ng of total RNA was reverse transcribed using a Superscript III kit (Invitrogen) and cDNAs were diluted 1:10. Specific PCR primers were designed using the NCBI Primer-Blast tool with mouse Col1a1 mRNA (NM_007742.3) as template: Col1a1 forward primer 5'-CTGCCCTCCTGACGCATGGC-3'; Col1a1 reverse primer 5'-AACGGGTCCCCTTGGGCCTT-3'. 4 μL cDNA (run in triplicates) was used as template in the subsequent qPCR reactions using a 2x SybrGreen MasterMix (Bioline) and an ABI 7900HT thermocycler (Applied Biosystems)..

Results

Confirmed engraftment by histology occurred in 8 WT mice and 9 TSP-2 KO mice. The CD31 quantification used 9 WT and 10 TSP-2 KO mice in which BrdU positive grafts were identified. 8 WT and 10 TSP-2 KO mice exhibited no BrdU-positive grafts, and were not included in the subsequent analysis. Cell viability (before injection) of grafted cells was about 90% for both TSP-2 KO and WT E14.5 cardiomyocytes. Of the stained adherent cells, 100% were BrdU-positive, and 95-100% were myosin-positive.. We grafted WT cardiomyocytes into WT recipients and TSP-2KO cardiomyocytes into TSP-2 KO recipients. The rationale behind this design is related to TSP-2 expression as this protein is produced primarily by fibroblasts and secondarily by macrophages. Since embryonic day 14.5 hearts, used here as donor tissue, contain little fibroblasts and we do not expect any TSP-2 production from the highly enriched grafted cardiomyocytes, we would not expect a different outcome if WT cells were grafted into TSP-2 KO recipients and vice versa.

We confirmed scar-localized TSP-2 expression in the injection-injured area of WT mice (Figure 1A, B). Grafted cells formed cadherin positive junctions with each other and with host cells (Figure 1C). Compared to WT mice, TSP-2 KO mice formed larger grafts (Figure 1D, E) that corresponded to a 46% increase in grafted cell number in the TSP-2 KO mouse (41±8 cells per 5 μm section for TSP-2 KO versus 28±5 cells in WT, $p<0.05$). Figure 1D and E show that BrdU-labeled embryonic cardiomyocyte grafts appropriately express sarcomeric myosin heavy chain, and arrange parallel to host tissue. Grafts similar in proximity to host tissue as shown in Figure 1D occurred in 8 of 9 TSP-2 KO mice but only in 2 of 8 WT mice. Cells injected into TSP-2 KO mice form several well-distributed grafts, but WT controls typically formed single grafts consisting of considerable necrotic cell debris.

WT mice formed twice as much scar around injected cells than TSP-2 KO mice. Collagen occupied 9.4±0.9% of total heart cross-sectional area for WT and 4.4±0.8% ($p<0.01$) of total area in TSP-2 KO mice. In addition, average scar thickness was 7-fold thinner ($p<0.01$) in TSP-2 KO mice compared to controls, and the ratio of scar area to graft area was 4.5 fold smaller ($p<0.05$) in TSP-2 KO mice (Figure 2). Specimens with the smallest graft thickness by these measurements, had the highest likelihood of exhibiting cadherin-rich intercellular junctions along the host-graft border (Figure 1C).

We used the endothelial marker, CD31 to test for an effect of TSP-2 deletion on vascularization (Figure 3). In TSP-2 KO mice, the percentage of graft injury area occupied by endothelial cells is 2.5 fold higher ($p<0.001$) than in WT mice. The vascular density as measured by a point-counting scheme is 60% more ($p<0.02$) in regions of TSP-2 KO graft injury, compared to that in WT mice.

Collagen type I alpha 1 (Col1a1) expression after grafting

Col1a1 expression was assessed in hearts of WT and TSP-2 KO mice after grafting of WT and TSP-2 KOneonatal cardiomyocytes, respectively. At 4 days after grafting, qPCR analysis revealed similar levels of Col1a1 mRNA expression in WT hearts grafted with WT cardiomyocytes compared to TSP-2 KO hearts grafted with TSP-2 KO cardiomyocytes (WT^{heart}/WT^{cardio} 1.0 ± 0.3 vs TSP-2 KO^{heart}/TSP-2 KO^{cardio} 1.1 ± 0.1). Since at this early time point (4 days) scar formation has not yet occurred, this result suggests that the host tissue rather than the engrafted cells account for the observed differences in the degree of fibrosis at the 2-week time point.

Discussion

We have identified a novel role for TSP-2 that could prove useful in cardiac repair. One persistent challenge of cell therapy in the heart is graft encapsulation by scar (4, 5). This is the first report of a single gene knockout improving conditions for graft survival, integration, and vascularization. These findings have important implications for understanding the heart's response to grafted cells and for future therapies to increase cardiac cell graft effectiveness. Loose collagen structure in the graft scar could permit grafted cardiomyocytes to form electromechanical junctions with the host more readily, while increased vascularity associated with a lack of TSP-2 could facilitate coronary perfusion of the grafts.

We grafted WT cardiomyocytes into WT recipients and TSP-2 KO cardiomyocytes into TSP-2 KO recipients. The rationale behind this design is related to TSP-2 expression as this protein is produced primarily by fibroblasts and secondarily by macrophages (10). Since embryonic day 14.5 hearts, used as donor tissue, contain little fibroblasts and we do not expect any TSP-2 production from the highly enriched grafted cardiomyocytes, we would not expect a different outcome if WT cells were grafted into TSP-2 KO recipients and vice versa. This is supported by qPCR for Col1a1 mRNA at an early time point (4 days) after grafting before scar formation has set in. Here, no differences in Col1a1 mRNA levels in the injected areas were observed, suggesting that the host tissue rather than the engrafted cells account for the observed differences in the degree of fibrosis at the later 2-week time point.

These results parallel the role TSP-2 plays in skin wound healing and in response to biomaterial implants. Kyriakides and colleagues found less organized collagen bundles and a 6-fold increased blood vessel density in the foreign body capsule in TSP-2 KO mice implanted with polymer biomaterials (7, 13). The cardiac scar encapsulating cell grafts resembles scar generated in foreign body reactions; both exhibit densely packed collagen fibers, low vascular density and a chronic local inflammatory response.

Grafts were found with equal frequency between the two groups, but the grafts in TSP-2 KO mice tended to be more numerous than in controls. This may be attributed to an underlying deficiency in collagen fibril formation, previously noted in connective tissues elsewhere (11, 12, 20), and in the heart (14, 15). Cells injected into knockout mice physically dissected the myocardium more easily than in the WT mice.

The basis for the TSP-2-related differences in scar formation has been previously shown to result from increased matrix metalloproteinase MMP2 and MMP9 activity in the absence of TSP-2 (10, 14, 21). TSP-2 binds MMP2, and the complex is then cleared from the extracellular space by binding to the lipoprotein receptor-related protein-1 (LRP-1) scavenger receptor (12). MMP2 is found at higher levels in injuries of TSP-2 KO mice (14), and has been implicated in abnormal collagen deposition. Thus, in the absence of TSP-2, levels of MMPs rise in the ECM and contribute to the degradation of fibrillar collagen.

Cell grafts form avascular clumps when initially injected, and are dependent on host angiogenesis for their long-term survival. The difference in blood vessel formation in this model can be explained by TSP-2's well-documented inhibition of endothelial cell proliferation (22, 23). The endothelial response in cell-engrafted TSP-2 KO mice is greater than in control mice, indicating TSP-2's role in limiting endothelial cell proliferation also applies to the heart.

We found that TSP-2 KO changes the nature of the heart's response to cardiac grafting in a manner consistent with observations in other wound healing models. TSP-2's previously identified role in collagen fiber formation and its ability to regulate MMP activity shed light on the mechanism of graft-induced cardiac fibrosis and suggest that clinical intervention could improve graft cell integration into the host. The significant difference in scar and vessel formation two weeks after cell engraftment suggests that a transient interference in TSP-2 protein production could create an environment in which grafts form electromechanical junctions with the host. After cell grafts are established, TSP-2 knockdown could be reversed or permitted to decay so that the potential long-term negative effects of reduced levels of TSP-2 could be avoided.

Acknowledgments

We thank Luz Linares for histology assistance,Jennifer Deem for surgery assistanceand Lil Pabon for insight in evaluating results.

Funding Sources

This work was supported by National Institutes of Health grants HL64387 (CEM), HL94374 (CEM), HL61553 (CEM), HL84642 (CEM), AR45418 (PB), T32 EB001650 (TER), T32 GM007266 (TER), and the University of Washington's Mouse Metabolic Phenotyping Center DK076126. TER also received funding from the ARCS Foundation and a Poncin Scholarship.

References

1. Klug MG, Soonpaa MH, Koh GY, Field LJ. Genetically selected cardiomyocytes from differentiating embronic stem cells form stable intracardiac grafts. J Clin Invest. Jul 1; 1996 98(1): 216–24. [PubMed: 8690796]
2. Ghostine S, Carrion C, Souza LC, Richard P, Bruneval P, Vilquin JT, et al. Long-term efficacy of myoblast transplantation on regional structure and function after myocardial infarction. Circulation. Sep 24; 2002 106(12 Suppl 1):I131–6. [PubMed: 12354722]
3. Stevens KR, Rolle MW, Minami E, Ueno S, Nourse MB, Virag JI, et al. Chemical dimerization of fibroblast growth factor receptor-1 induces myoblast proliferation, increases intracardiac graft size,

and reduces ventricular dilation in infarcted hearts. Hum Gene Ther. May; 2007 18(5):401–12. [PubMed: 17518610]

4. Reinecke H, Zhang M, Bartosek T, Murry CE. Survival, integration, and differentiation of cardiomyocyte grafts: a study in normal and injured rat hearts. Circulation. Jul 13; 1999 100(2): 193–202. [PubMed: 10402450]
5. Laflamme MA, Chen KY, Naumova AV, Muskheli V, Fugate JA, Dupras SK, et al. Cardiomyocytes derived from human embryonic stem cells in pro-survival factors enhance function of infarcted rat hearts. Nat Biotechnol. Sep; 2007 25(9):1015–24. [PubMed: 17721512]
6. Brower GL, Gardner JD, Forman MF, Murray DB, Voloshenyuk T, Levick SP, et al. The relationship between myocardial extracellular matrix remodeling and ventricular function. Eur J Cardiothorac Surg. Oct; 2006 30(4):604–10. [PubMed: 16935520]
7. Kyriakides TR, Leach KJ, Hoffman AS, Ratner BD, Bornstein P. Mice that lack the angiogenesis inhibitor, thrombospondin 2, mount an altered foreign body reaction characterized by increased vascularity. Proc Natl Acad Sci U S A. Apr 13; 1999 96(8):4449–54. [PubMed: 10200282]
8. Kyriakides TR, Tam JW, Bornstein P. Accelerated wound healing in mice with a disruption of the thrombospondin 2 gene. J Invest Dermatol. Nov; 1999 113(5):782–7. [PubMed: 10571734]
9. Bornstein P, Armstrong LC, Hankenson KD, Kyriakides TR, Yang Z. Thrombospondin 2, a matricellular protein with diverse functions. Matrix Biol. Dec; 2000 19(7):557–68. [PubMed: 11102746]
10. Agah A, Kyriakides TR, Letrondo N, Bjorkblom B, Bornstein P. Thrombospondin 2 levels are increased in aged mice: consequences for cutaneous wound healing and angiogenesis. Matrix Biol. Jan; 2004 22(7):539–47. [PubMed: 14996433]
11. Kyriakides TR, Zhu YH, Smith LT, Bain SD, Yang Z, Lin MT, et al. Mice that lack thrombospondin 2 display connective tissue abnormalities that are associated with disordered collagen fibrillogenesis, an increased vascular density, and a bleeding diathesis. J Cell Biol. Jan 26; 1998 140(2):419–30. [PubMed: 9442117]
12. Bornstein P, Agah A, Kyriakides TR. The role of thrombospondins 1 and 2 in the regulation of cell-matrix interactions, collagen fibril formation, and the response to injury. Int J Biochem Cell Biol. Jun; 2004 36(6):1115–25. [PubMed: 15094126]
13. Kyriakides TR, Hartzel T, Huynh G, Bornstein P. Regulation of angiogenesis and matrix remodeling by localized, matrix-mediated antisense gene delivery. Mol Ther. Jun; 2001 3(6):842–9. [PubMed: 11407897]
14. Schroen B, Heymans S, Sharma U, Blankesteijn WM, Pokharel S, Cleutjens JP, et al. Thrombospondin-2 is essential for myocardial matrix integrity: increased expression identifies failure-prone cardiac hypertrophy. Circ Res. Sep 3; 2004 95(5):515–22. [PubMed: 15284191]
15. Cleutjens JP, Blankesteijn WM, Daemen MJ, Smits JF. The infarcted myocardium: simply dead tissue, or a lively target for therapeutic interventions. Cardiovasc Res. Nov; 1999 44(2):232–41. [PubMed: 10690298]
16. Rysa J, Leskinen H, Ilves M, Ruskoaho H. Distinct upregulation of extracellular matrix genes in transition from hypertrophy to hypertensive heart failure. Hypertension. May; 2005 45(5):927–33. [PubMed: 15837839]
17. Sezaki S, Hirohata S, Iwabu A, Nakamura K, Toeda K, Miyoshi T, et al. Thrombospondin-1 is induced in rat myocardial infarction and its induction is accelerated by ischemia/reperfusion. Exp Biol Med (Maywood). Oct; 2005 230(9):621–30. [PubMed: 16179730]
18. Virag JI, Murry CE. Myofibroblast and endothelial cell proliferation during murine myocardial infarct repair. Am J Pathol. Dec; 2003 163(6):2433–40. [PubMed: 14633615]
19. Robey TE, Murry CE. Absence of regeneration in the MRL/MpJ mouse heart following infarction or cryoinjury. Cardiovasc Pathol. Jan-Feb;2008 17(1):6–13. [PubMed: 18160055]
20. Kyriakides TR, Zhu YH, Yang Z, Bornstein P. The distribution of the matricellular protein thrombospondin 2 in tissues of embryonic and adult mice. J Histochem Cytochem. Sep; 1998 46(9):1007–15. [PubMed: 9705966]
21. Agah A, Kyriakides TR, Bornstein P. Proteolysis of cell-surface tissue transglutaminase by matrix metalloproteinase-2 contributes to the adhesive defect and matrix abnormalities in

thrombospondin-2-null fibroblasts and mice. Am J Pathol. Jul; 2005 167(1):81–8. [PubMed: 15972954]

22. Armstrong LC, Bjorkblom B, Hankenson KD, Siadak AW, Stiles CE, Bornstein P. Thrombospondin 2 inhibits microvascular endothelial cell proliferation by a caspase-independent mechanism. Mol Biol Cell. Jun; 2002 13(6):1893–905. [PubMed: 12058057]
23. Oganesian A, Armstrong LC, Migliorini MM, Strickland DK, Bornstein P. Thrombospondins use the VLDL receptor and a nonapoptotic pathway to inhibit cell division in microvascular endothelial cells. Mol Biol Cell. Feb; 2008 19(2):563–71. [PubMed: 18032585]

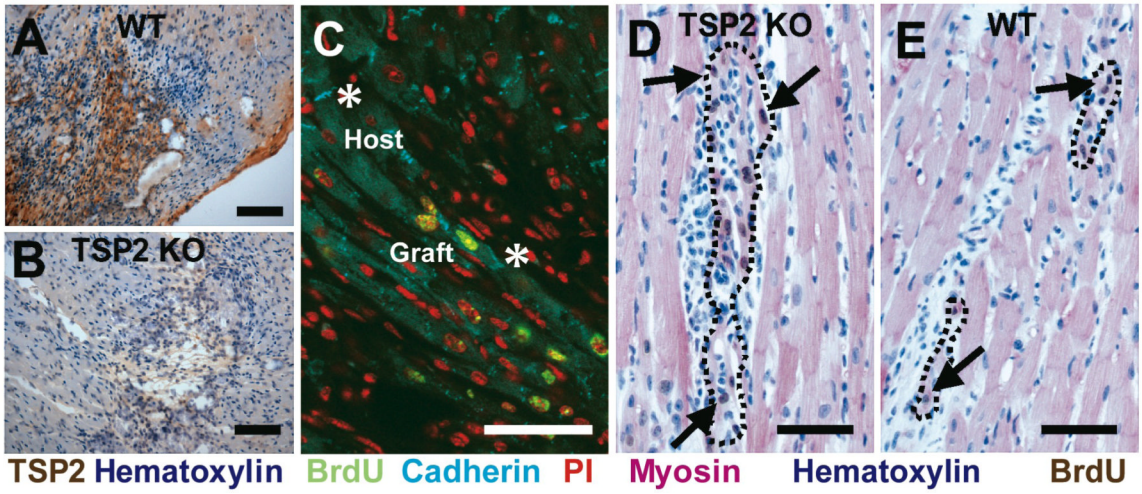

Figure 1. TSP-2 expression and graft integration

Transplanted E14.5 cardiomyocytes express TSP-2 two weeks after engraftment in WT mouse hearts (A), but not in TSP-2 KO mice (B) (Bars=100 μm). (C) Confocal microscopy. Grafted cardiomyocytes (green nuclei) express cadherin (teal) and form cell junctions with each other and with host cells (asterisks). Propidium iodide was used as nuclear counterstain (red) (Bar=50μm). (D) BrdU (brown; arrows) labeled E14.5 cardiomyocytes express sarcomeric myosin (red), exhibit close apposition to host cardiomyocytes, and form larger grafts (outlined) in TSP-2 KO mice compared to WT controls (E). (Bar=50 μm)

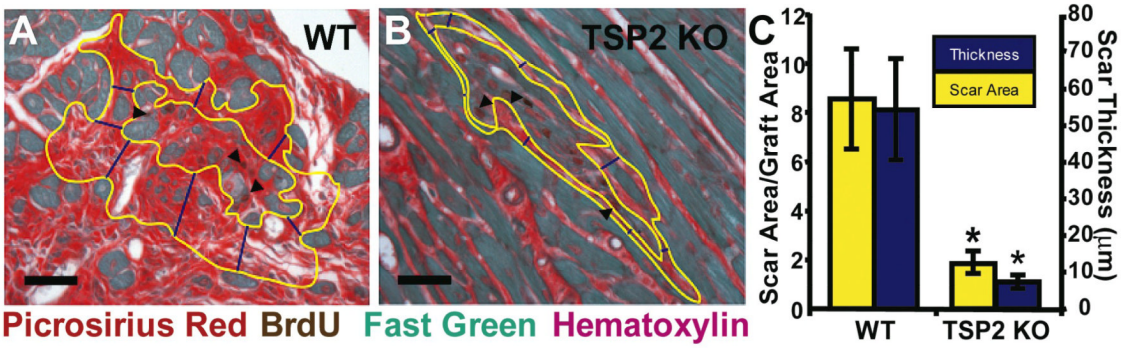

Figure 2. Effects of TSP-2 knockout on peri-graft fibrosis

(A) Grafted cardiomyocytes (arrowheads) in WT hearts elicit a vigorous collagen scar response compared to TSP-2 KO mice (B), which generate much less fibrosis. (Bars=50 μm). There are 4.5-fold and 7-fold differences (C) in scar area (outlined in yellow) and thickness (measured in blue), respectively, between WT and TSP-2 KO mice (* $p<0.05$).

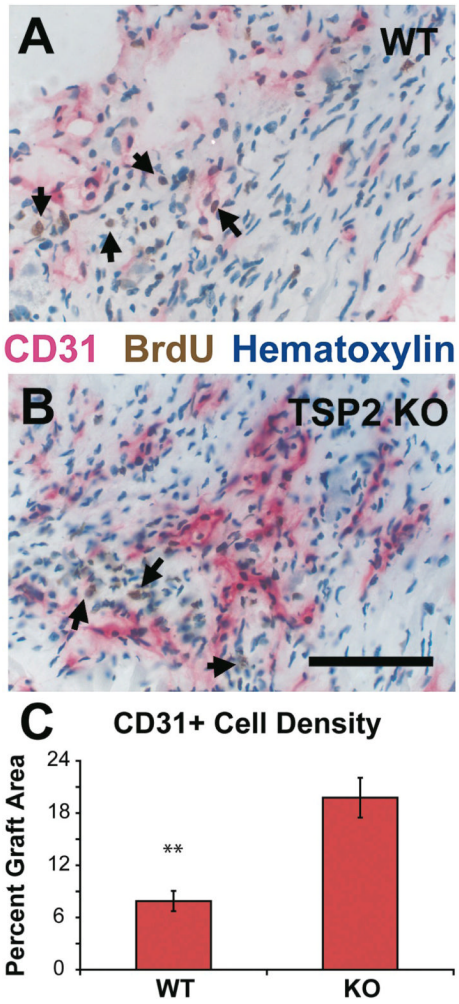

Figure 3. Effect of TSP-2 knockout on peri-graft vascularization

BrdU-labeled cardiomyocytes (arrows) elicit more CD31+ blood vessels in TSP-2 KO mice (B) than in WT controls (A) (Bar=100 μm). Morphometry indicated a 2.5-fold increase in total endothelial cell area in TSP-2 KO hearts (C) (** $p<0.001$).

Table 1

Study groups and survival rates.

Groups	Recipient Genotype	noperated/n survivors	% survival
Wildtype sham (saline)	Wildtype	10/8	80%
TSP2-KO sham (saline)	TSP2-KO	10/8	80%
Wildtype (WT cardios)	Wildtype	32/26	81%
TSP2-KO (TSP2-KO cardios)	TSP2-KO	35/29	83%
Wildtype sham (no injection for baseline)	Wildtype	5/5	100%
TSP2-KO sham (no injection for baseline)	TSP2-KO	5/4	80%
Wildtype (WT cardios for PCR)	Wildtype	8/6	75%
TSP2-KO (TSP2-KO for PCR)	TSP2-KO	10/6	60%
Total Wildtype mice		55/45	82%
Total TSP-KO mice		60/47	78%